Computational Research Progress in Applied Science & Engineering

ISSN 2423-4591

CRPASE Vol. 05(01), 10-15, March 2019

State-of-the-art Noise Suppression Methods: A Complete Review

Noorbakhsh Amiri Golilarz[a*], Ahmad Karambakhsh[b], Amin Salehpour[c]

[a] *School of Computer Science and Engineering, University of Electronic Science and Technology of China, China*
[b] *Department of Electrical Engineering, Shanghai Jiao Tong University, China*
[c] *Department of Electrical and Electronic Engineering, Eastern Mediterranean University, Cyprus*

Keywords

Image de-noising,
Important characteristics,
Small noisy coefficients,
3D transform domain.

Abstract

Many ideas have been implemented for image de-noising and some of these techniques act properly in noise discarding. In this paper, a review of some state-of-the-art noise suppression methods has been presented. These methods were introduced to develop some new strategies to reduce the noise effect from the images by keeping the most important characteristics and discarding small noisy coefficients. In addition, these techniques were conducted to overcome the performance analysis of the previous approaches in terms of acquiring higher Peak Signal to Noise Ratio (PSNR) and to improve the visual quality of the images. In this study, six state-of-the-art unique techniques for image de-noising have been reviewed and their performances have been analyzed. Results show that de-noising based on sparse 3D transform-domain collaborative filtering performs well in comparison with other techniques.

1. Introduction

Image de-noising is among the essential roles to accurate the imperfections produced during transmitting and receiving procedures. Therefore some succeeding processes like image analyzing may not be possible until doing suitable noise repression techniques to improve the quantitative and visual inspection if image.

Discarding the noise while keeping the most important characteristics of the images is still a challenging problem for researchers in image processing and many methods have been proposed. Donoho and Johnstone proposed ideal spatial adaptation by wavelet shrinkage [1]. X. P. Zhang introduced thresholding neural network for adaptive noise reduction [2]. Noorbakhsh Amiri Golilarz and Hasan Demirel suggested to use thresholding neural network (TNN) based noise reduction with a new improved thresholding function [3]. Translation invariant wavelet based noise reduction using a new smooth nonlinear improved thresholding function is introduced in a study conducted by Noorbakhsh Amiri Golilarz et al., in 2017 [4]. In 2017 Gabriela Ghimpe¸teanu et al., proposed a decomposition framework for image de-nosing algorithm [5]. Jiefei Wanget al., developed a residual based kernel regression method for image de-noising [6]. Image super-resolution via sparse representation is introduced by Jianchao Yang et al., in 2010 [7]. Image de-noising based on improved wavelet threshold function for wireless camera networks and transmissions is suggested by Xiaoyu Wang et al., in 2015 [8]. Kostadin Dabov et al., proposed image de-noising by sparse 3D transform-domain collaborative filtering in 2007 [9]. Space scale adaptive noise reduction based on thresholding neural network was conducted in a study proposed by X. P. Zhang in 2001 [10].

In this research, we presented a review of some state-of-the-art noise repression methods. These methods were proposed to develop some new strategies to obtain desired de-noised images by discarding the noise from the images while keeping the fine details. Here performance analysis and visual quality of several state-of-the-art image de-noising methods have been analyzed and also the experimental results have been compared.

2. Noise

An image can be contaminated by noise during receiving and transmitting processes. This noise can be as Additive White Gaussian Noise (AWGN) which can corrupt the image and leads toward diminishing its visual quality. Eq.(1) denotes the effect of noise on original images.

$$v = p + \varepsilon \qquad (1)$$

where p is the noise free image, ε is the noise which it can be Additive White Gaussian Noise (AWGN) with zero mean and standard deviation of σ and v is the noisy image.

The main objective in image de-noising is discarding the noise from images to improve the resolution, obtain higher

* Corresponding Author:
E-mail address: noorbakhsh.amiri90@gmail.com

Received: 30 September 2018; Accepted: 10 December 2018

Peak Signal to Noise Ratio (PSNR) and minimize the Mean Square Error (MSE) [11].

3. State-of-the-art Image De-noising Techniques

A. A Decomposition Framework for Image De-noising Algorithms

In this technique, Gabriela Ghimpeteanu et al., suggested to use a decomposition framework for noise suppression [5]. In this proposed technique, the constituents of the image should be calculated properly to be utilized in a moving frame encrypting its local geometry [5]. To conserve gradients directions and level lines, the constituents of the image must be de-noised well in the moving frame [5].

Regarding to a scaled variant ρJ of J , it is possible to parametrize its diagram using the Eq. (2)

$$\partial: (x, y) \rightarrow (x, y, \rho J\,(x, y)) \tag{2}$$

where $\rho \in [0, 1]$, A is the surface in R^3 , (x, y) is the typical norm system of R^2 , $J : \varphi \subset R^2 \rightarrow R$ is a gray-level image, J_x is derivative of J in x direction, J_y is derivative of J in y direction and finally, the gradient of J *is* denoted by ∇J [5].

Figure 1 shows the orthonormal moving frame (Z_1, Z_2, N) [5]. In this figure, the vector field Z_1 denotes to the tangent of the surface A signifying the steepest slope direction at every specific location in the surface A, the vector field Z_2 is tangent to the surface A signifying the lowest slope direction at every specific location in the surface A and N is normal to the surface A. Z_1 , Z_2 can be obtained by Eq. (3) [5]

$$Z_1 = \frac{d\partial(z_1)}{\|d\partial(z_1)\|_2},\ Z_2 = \frac{d\partial(z_2)}{\|d\partial(z_2)\|_2} \tag{3}$$

where d_∂ denotes to the differential of ∂.

Additionally, figure 1 shows the local geometry of gray level image with the encrypting of moving frame. In this figure, left image is the original gray-level image and (Z_1, Z_2) is the moving frame and also we can observe the gradient direction and the level-line of the image at points p and q of the image domain φ [5]. Besides, right image shows the orthonormal moving frame (Z_1, Z_2, N) signifying the steepest and lowest slopes direction of the surface A [5].

These vector fields Z_1, Z_2, N can be expressed in details by the matrix field K using Eq. (4) [5]

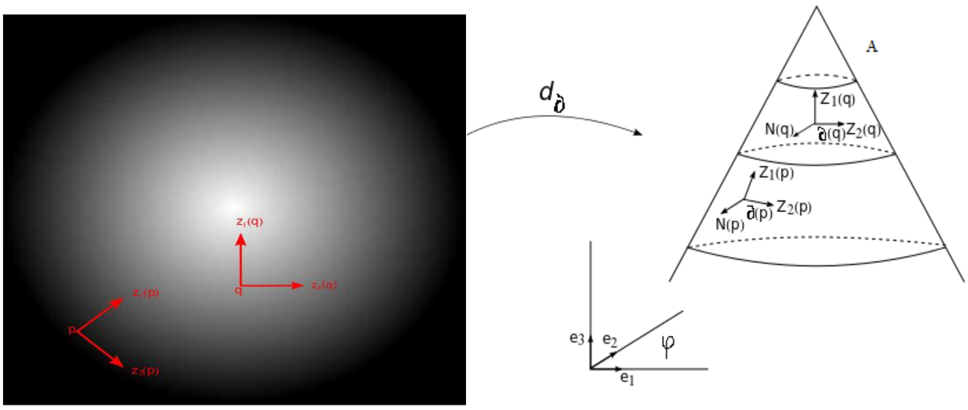

Figure 1. The Local Geometry of A Gray-level Image Combined with Encoding of Moving Frame [5].

$$K=\begin{pmatrix} \frac{J_x}{\sqrt{\nabla J^2(1+\rho^2|\nabla J|^2)}} & \frac{-J_y}{|\nabla J|} & \frac{-\mu J_x}{\sqrt{1+\rho^2|\nabla J|^2}} \\ \frac{I_x}{\sqrt{\nabla J^2(1+\rho^2|\nabla J|^2)}} & \frac{-J_x}{|\nabla J|} & \frac{-\mu J_y}{\sqrt{1+\rho^2|\nabla J|^2}} \\ \frac{\mu|\nabla J|^2}{\sqrt{\nabla J^2(1+\rho^2|\nabla J|^2)}} & 0 & \frac{1}{\sqrt{1+\rho^2|\nabla J|^2}} \end{pmatrix} \tag{4}$$

where the reference points of the vector fields Z_1 , Z_2 and N are in the first, second and third columns, respectively.

In Figure 1, regarding to $e_1 = (1, 0, 0)$, $e_2 = (0, 1, 0)$, $e_3 = (0, 0, 1)$ which are the orthonormal frame of $(R^3, \|\ \|2)$, the K in Eq.(4) is the frame change field which varies from (e_1, e_2, e_3) to (Z_1, Z_2, N). It is clear that the R^3numerical quantitative functions constituents $(0, 0, J)$ can be referred to (l^1, l^2, l^3) in the new frame which is formulated by Eq. (5) [5]

$$\begin{pmatrix} 0 \\ 0 \\ J \end{pmatrix} = K \begin{pmatrix} l^1 \\ l^2 \\ l^3 \end{pmatrix} \tag{5}$$

The process of obtaining output de-noised image is as the following [5]:

Step 1. Apply suitable de-noising technique to reduce the effect of noise while keeping the most important characteristics of image.

Step 2. Obtain J constituents (l^1, l^2, l^3) for different scalars of ρ.

Step 3. Apply same suitable de-noising technique to the existing constituents to get the de-noised constituents $(l^1{}_{den}, l^2{}_{den}, l^3{}_{den})$

Step 4. Apply the inverse frame change matrix field (ω) to the new de-noised constituents:

$$\begin{pmatrix} l^1{}_{den} \\ l^2{}_{den} \\ l^3{}_{den} \end{pmatrix} = K^{-1} \begin{pmatrix} J^1{}_{den\omega} \\ J^2{}_{den\omega} \\ J^3{}_{den\omega} \end{pmatrix} \tag{6}$$

where components $J^1{}_{den\omega}$, $J^2{}_{den\omega}$ and $J^3{}_{den\omega}$are the first, second and third component which are marked by $J_{den\omega}$

Step 5. Get output de-noised image J_{den}

Step 6. Compare J_{den} and $J_{den\omega}$ with based on *PSNR* values.

B. A Residual-Based Kernel Regression Method for Image Denoising

Wang et al., in 2016 proposed a residual-based method for removing the noise from images contaminated by Gaussian noise [6]. Combination of bilateral filter and structure adaptive kernel filter as well as the image residuals results in repressing the noise effectively while the excellent features, such as edges, can be preserved [6].

The procedure of this technique is as follows:

Step 1. Obtain the reconstructed image V_2 by restoring the noisy image g with bilateral filter utilizing Eq. (7)

$$\hat{e}_i = v(p_i) - V(p_i),\ i=0,1,\ldots,L \tag{7}$$

where $V(p_i)$ is the pixel value at point p_i of the noise free image, L is the number of pixels, $v(p_i)$ is pixel value at point p_i of noisy image and $\hat{e}_i$ is image residual.

Step 2. Setting a standard for image residual according to Eq. (8)

$$Q(p_i) = \sum_{w\in M_{n1}(p_i)} \hat{e}_i,\ i=1,\ldots,L \tag{8}$$

where M_{n1} refers to the neighbor of p_i with radius of $n1$.

Step 3. Tagging abnormal points using Eq. (9)

$$Z_1(p_i) = \begin{cases} 1, \mathrm{Q}(p_i) < \varphi_1\ or\ \mathrm{Q}(p_i) > \varphi_2 \\ 0, \quad otherwise \end{cases} \tag{9}$$

where φ value is used for tagging intensity [6].

If noise still exists, for a tagged residual figure $Z_1(p_i)$, it should be filtered again as Eq. (10)

$$Z_2(p_i) = \begin{cases} 1,\ \sum_{\mathrm{t}\in M_{n2}(p_i)} Z_1(\mathrm{t}) > \tau_1,\ Z_1(p_i) = 1 \\ 0, \quad otherwise \end{cases} \tag{10}$$

where τ_1 is a defined threshold and M_{n2} refers to the neighbor of p_i with radius of $n2$.

This process continues to decrease the noise distribution in the tagged image (Eq. (11)). This step results in getting the binary image.

$$Z_3(p_i) = \begin{cases} 1,\ \sum_{\mathrm{t}\in M_{n3}(p_i)} Z_2(\mathrm{t}) > \tau_2,\ Z_2(p_i) = 1 \\ 0, \quad otherwise \end{cases} \tag{11}$$

Specifically, let *V1* be de-noised image using structure adaptive kernel method and *V2* be the de-noised image by bilateral filter. Then the output image *V3* can be obtained using Eq. (12) [6]

$$V_3(p) = Z_3(p)\, V_1(p) + (1 - Z_3(p))\, V_2(p) \tag{12}$$

Additionally, to remove the image edges it is better to use the improved smoothed version of Eq. (12) according to the following formula.

$$Z'_3(p_i) = \begin{cases} 0.3,\ \sum_{t\in M_2(p_i)} Z_3(t) \neq \#\, M_2(p_i),\ Z_3(p_i) = 1 \\ 0, \quad otherwise \end{cases} \tag{13}$$

where $\# M_2$ refers to the quantity of components of set M_2

Step 4. Suppress the noise from pixels at point p_i of noisy image v which satisfies the first restriction of Eq. (11) and get V_1 by employing the structure adaptive based method.

Step 5. Obtain reconstructed noise free image V_3 according to the following formula:

$$V_3(p) = Z'_3(p)\, V_1(p) + (1 - Z'_3(p))\, V_2(p) \tag{14}$$

C. Image super resolution via sparse representation

In this study, Yang et al., introduced sparse signal representation for a single-image super resolution. This study shows that it is possible to define the patches of an image as a sparse linear combination of components from a suitably chosen over-complete dictionary. Regarding to this observation, a sparse representation for each patch of the low-resolution input is needed to utilize the coefficients of this representation to produce the high-resolution output. Training two dictionaries together for the both high and low resolution patches of an image provides us with compelling the sparse representations resemblance among the patches of an image with high and low resolution regarding to their own dictionaries. Then it is possible to obtain a high resolution patch of an image by employing the sparse representation of a low resolution patch of an image with the dictionary of the high resolution patch of an image. The whole procedure to obtain a super resolution image is as following [7]:

Step 1. Train U_h and U_l dictionaries.

Step 2. For each patch *z* of *Z*

Step 2.1. Calculate mean pixel value *M* of patch *z*

Step 2.2. Find a solution for the following optimization problem.

$$min_\gamma \left\|\tilde{U}\gamma - \tilde{z}\right\|^2{}_2 + \rho\|\gamma\|_1 \tag{15}$$

Step 2.3. Get the high-resolution patch $k = U_h\ \gamma^*$. Utilize the patch $k + M$ into a high-resolution image K_0.

Step 3. Obtain the closest image to X_0 satisfying the reconstruction constraint based on gradient descent as Eq. (16)

$$K^* = argmin_k \|SHK - Z\|^2{}_2 + c\|K - K_0\|^2{}_2 \tag{16}$$

Step 4. Generate K^* as the super resolution image.

Here *K, Z, k* and *z* are high resolution image, low resolution image, high resolution image patch and low resolution image patch, respectively. U is dictionary for sparse coding (U_h is dictionary for high resolution patch of an image and U_l is dictionary for low resolution patch of an image) and S is down sampling operator. *H* is blurring filter. In addition, to stable the sparsity of the solution and accuracy of the approximation to *z*, parameter ρ is used. γ is the sparse representation [7].

D. Image De-noising Based on Improved Wavelet Threshold Function for Wireless Camera Networks and Transmissions

In 2014, Wang et al., proposed wavelet based threshold function for image de-noising. This function is given by Eq. (17) [8]

$$q = \begin{cases} sign(f)\left[|f| - sin(\frac{\pi}{2}\left|\frac{\theta}{f}\right|^m)\,\theta\right], |f| > \theta \\ 0 \quad , |f| < \theta \end{cases} \tag{17}$$

where *q* is the threshold function, *f* is wavelet coefficient, *m* is the adjustment parameter and θ is threshold value.

The proposed method can be processed as follows [8]:

Step 1. Add Gaussian White Noise

Step 2. Decompose the noisy image

Step 3. Apply improved thresholding function to de-noise the image

Step 4. Reconstruct image with wavelet coefficients obtained from the proposed wavelet based threshold function.

E. Image De-noising by Sparse 3D Transform-domain Collaborative Filtering

In this study, Dabov et al., proposed a unique approach for discarding the noise from images in transform domain based on an enhanced sparse representation [9]. Assembling segments of the similar two dimensional (2D) image into three dimensional (3D) group results in sparsity improvement. To handle these 3D groups, a cooperative filtering should be developed. To do so, the following sequential steps are needed: three dimensional transformation of a group, shrinkage of the transform spectrum and inverse 3D transformation [9]. These procedures will result in a three dimensional estimate including the jointly filtered grouped image blocks [9]. Noise diminishing provides us with revealing the finest details distributed by grouped blocks and also conserving most important singular characteristics of a particular block by cooperative filtering. Then filtered blocks will get back to their initial posture. Subsequently, a lot of distinctive estimates can be acquired for each individual pixel due to the overlapping process of the blocks. A crucial enhancement will be obtained using a specific improved cooperative wiener filtering. This noise reduction strategy is implemented in 2 stages as follows [9]:

Stage 1: Basic estimate. Firstly, block-wise estimates: in the noisy image it is necessary to do grouping and collaborative hard thresholding for each block. In grouping, it is needed to find blocks resembling to the presently processed one and then collect them in three dimensional groups. In collaborative hard thresholding, we should apply a 3D transform to the formed group, perform hard thresholding to attack the noisy components and diminish the noise, apply inverse 3D transform to get estimation of all grouped blocks and finally return these estimations to their initial posture [9].

Secondly, aggregation: The basic estimate of the true image should be computed using weighted averaging all of the acquired overlapping block-wise estimates [9].

Stage 2: Final estimate. To perform enhanced grouping and cooperative wiener filtering exploiting the basic estimate [9].

Firstly, block-wise estimate: For each individual block we should do grouping and collaborative wiener filtering. In grouping, Block Matching (BM) should be utilized during the basic estimate to discover the position of the blocks resembling to the most recent processed one. Employing these positions provides us to form noisy image and basic estimate. In collaborative wiener filtering, 3D transform is employed on both groups namely, noisy image and basic estimate. Wiener filtering combined with energy spectrum of basic estimate acts as the true energy spectrum on the noisy image. Applying the inverse 3D transform on the filtered coefficients leads to getting estimates of all grouped blocks then returning these estimates to their initial stage [9].

Secondly, Aggregation: aggregate all of the acquired estimates with a weighted average to get a final estimate of the true image [9].

The mentioned algorithm is shown in Figure 2.

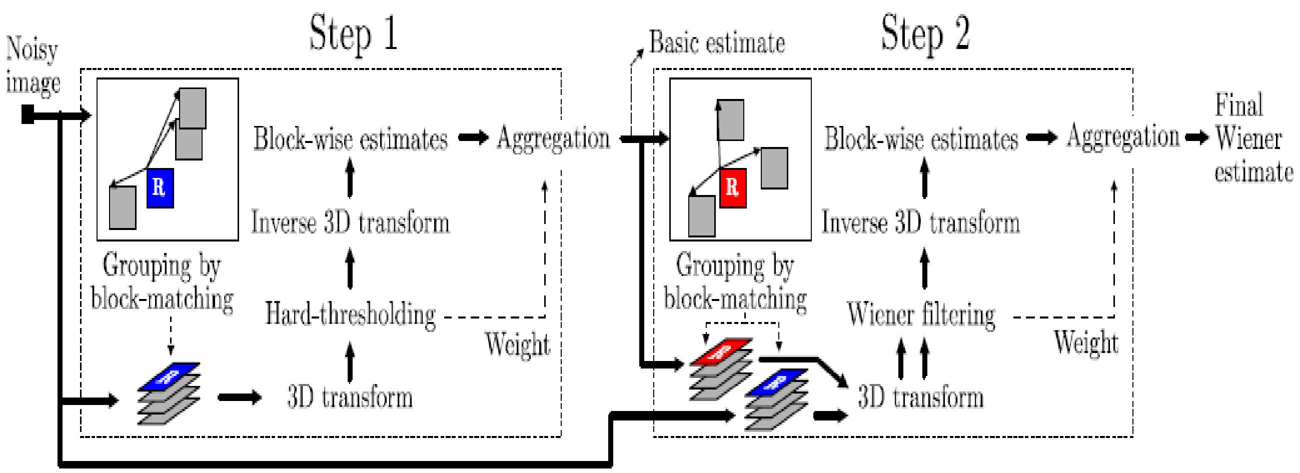

Figure 2. Flowchart of Image De-noising with Sparse 3D Transform-domain Collaborative Filtering [9].

F. Space Scale Adaptive Noise Reduction Based on TNN

This technique is adaptive because the two dimensional discrete wavelet transform (2D-DWT) is adopted as the linear transform in Thresholding Neural Network (TNN) and the noisy image acts as the input of this TNN [10]. In this structure, the input is noisy image and the transform can be orthogonal wavelet transform. Applying this linear transform results in wavelet coefficients contaminated by Gaussian noise. Then wavelet thresholding function can be employed to get noise reduced components. Finally, using inverse wavelet transform, it is possible to acquire desired reconstructed image.

Data stream with one dimensional coefficient including the space-scale data of two dimensional images should be prepared in order to get space scale adaptive noise repression image [10]. In this stage, the components of two dimensional discrete wavelet transform (2-D DWT) are reorganized as a series of one dimensional component in spatial order then the adjoining samples show exactly the same local areas in the original image [10]. Figure 3 shows this rearrangement process of an 8.8 transformed image properly [10]. The discrete wavelet transform of an image includes of 4 frequency channels namely, HH, HL, LH and LL which "H" refers to high frequency and "L" refers to low frequency. The decomposition levels can be done in LL channel as it is shown in Figure 3 (a). As it is shown in Figure 3 (b), all of these frequency channels contain different numbers which are called spatial order of two dimensional components referring to their specific positions in Figure 3 (a) [10].

4. Experimental Results

In this part a comparison between some state-of-the-art image de-noising methods has been done to understand their performance analysis and visual quality better in terms of discarding the noise from images. Sym4 wavelet with

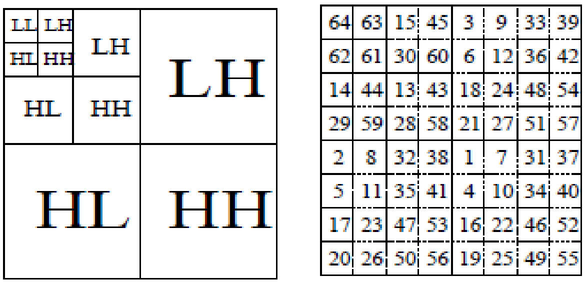

(a) (b)

Figure 3. Data Preparation of Image [10].

four level of decomposition has been used in both experiments. In the first experiment, 7 test images have been used with the size of 256× 256 and standard deviations of 5, 10, 15, 20, 25.

Table 1 shows the performance of 6 state-of-the-art de-noising techniques for average of 10 experiments. In this table, for each standard deviation, top left: image de-noising based on improved wavelet threshold function for wireless camera networks and transmissions, top right: space scale adaptive noise reduction based on TNN , mid left: a residual-based kernel regression method for image de-noising , mid right: image super resolution via sparse representation , bottom left: a decomposition framework for image de-noising algorithms and bottom right: image de-noising by sparse 3D transform-domain collaborative filtering .In most of the tests, we observe the superiority of de-noising by sparse 3D transform-domain collaborative filtering over other de-noising techniques.

Besides, in the second experiment, we used 'Lena' image with the size of 256× 256 and standard deviation of 15. In this experiment, we compared the visual quality of different de-noising methods. In Figure 4, (a) is de-noised image using improved wavelet threshold function for wireless camera networks and transmissions, (b) is de-noised image based on space scale adaptive noise reduction using TNN, (c) is de-noised image using residual-based kernel regression method, (d) is de-noised image based on super resolution via sparse representation, (e) is a de-noised image using decomposition framework and (f) is de-noised image using sparse 3D transform-domain collaborative filtering. As we can see in this figure, de-noising based on sparse 3D transform-domain collaborative filtering outperforms other alternative methods available in the literature.

Table 1. PSNR results for different state-of-the-art de-noising methods for average of 10 experiments.

Image	σ=5		σ=10		σ=15		σ=20		σ=25	
	38.29	38.53	34.18	33.78	31.91	32.36	30.48	30.54	29.45	29.81
C.man	38.36	37.42	34.24	34.07	32.01	32.31	30.50	30.36	29.78	29.22
	38.55	**39.02**	34.78	**35.12**	33.45	**33.65**	32.12	**32.85**	29.33	**29.98**
	39.83	39.99	36.71	36.87	34.94	35.15	33.77	33.83	32.86	32.95
House	40.12	39.45	36.67	36.76	34.91	34.12	33.90	33.93	32.82	33.07
	40.54	**41.10**	38.12	**38.42**	37.23	**37.76**	35.49	**35.96**	34.28	**34.69**
	38.12	38.30	34.68	34.67	32.70	32.94	31.29	31.34	30.16	30.43
Peppers	38.35	38.65	34.82	34.63	32.87	32.68	31.39	31.28	29.78	30.13
	38.46	**38.86**	37.12	**37.89**	35.42	**36.21**	33.20	**33.85**	32.35	**32.80**
	38.72	38.82	35.93	36.02	34.27	34.42	33.05	33.14	32.08	32.22
Lena	38.85	38.42	35.90	35.87	34.21	34.32	33.08	33.09	32.54	32.17
	38.90	**39.24**	38.69	**38.97**	37.16	**37.96**	36.09	**36.68**	34.58	**34.89**
	38.31	38.34	34.98	32.89	33.11	33.30	31.78	29.98	30.72	28.99
Barbara	38.54	38.64	35.23	35.05	33.32	32.01	32.10	31.84	31.56	30.15
	38.78	**39.04**	37.14	**37.87**	**35.47**	32.81	**33.17**	32.35	32.06	**32.67**
	37.28	37.47	33.92	33.87	32.14	32.29	30.88	30.98	29.91	30.03
Boats	37.36	37.65	33.91	33.78	32.09	32.36	30.81	30.72	29.45	29.81
	37.85	**38.12**	35.53	**36.24**	35.11	**35.80**	**33.45**	33.05	31.46	**31.95**
	37.14	37.30	33.62	32.56	31.86	32.05	30.72	30.98	29.85	29.96
Hill	37.45	37.18	33.67	33.53	31.85	31.93	30.68	30.56	30.12	29.64
	37.38	**38.31**	35.15	**36.12**	34.46	**35.21**	33.29	**34.11**	32.37	**32.86**

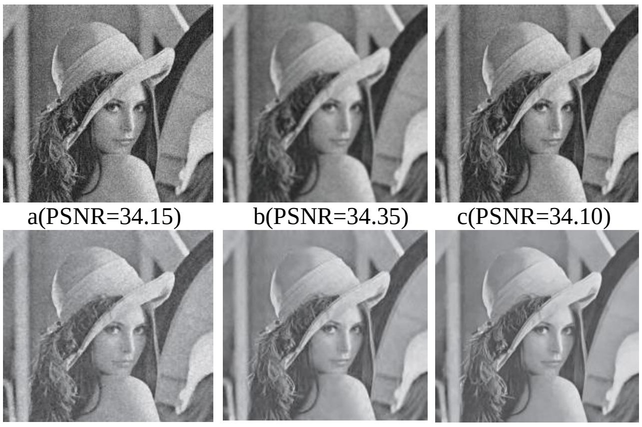

a(PSNR=34.15) b(PSNR=34.35) c(PSNR=34.10)

d(PSNR=34.27) e(PSNR=37.01) f(PSNR=37.88)

Figure 4. Lena Image De-noising for Different State-of-the-art Techniques for Standard Deviation of 15.

5. Conclusion

Researchers proposed many methods to discard the noise from the images where some of them perform well in removing the noise and obtaining output de-noised images. In this study, we introduced a review of some state-of-the-art noise reduction methods. These methods were developed to keep the most significant features of images and discard the noisy components. Performances of these techniques show their superiority over previous published methods in image de-noising. In this corresponding, a comparison has been done among some of the state-of-the-art image de-noising methods and results indicated the superiority of sparse 3D transform-domain collaborative filtering over other alternatives in the literature.

References

[1] D.L. Donoho, I.M. Johnstone, Ideal Spatial Adaptation by Wavelet Shrinkage, Biometrika 81 (1993) 425–455.

[2] X. P. Zhang, Thresholding Neural Network for Adaptive Noise Reduction, IEEE Transactions on Neural Networks 12 (2001) 567–584.

[3] Noorbakhsh Amiri Golilarz and Hasan Demirel, Thresholding Neural Network (TNN) Based Noise Reduction with a New Improved Thresholding Function, Computational Research Progress in Applied Science and Engineering (CRPASE) 3 (2017) 81–84.

[4] Noorbakhsh Amiri Golilarz, Niyifasha Robert, Jalil Addeh and Amin Salehpour, Translation Invariant Wavelet Based Noise Reduction using a New Smooth Nonlinear Improved Thresholding Function, Computational Research Progress in Applied Science and Engineering (CRPASE) 3 (2017) 104–108.

[5] Gabriela Ghimpe¸teanu, Thomas Batard, Marcelo Bertalmío and Stacey Levine, A Decomposition Framework for Image De-noising Algorithm, IEEE Transaction on Image Processing 25 (2016) 388–399.

[6] Jiefei Wang, Yupeng Chen, Tao Li, Jian Lu and Lixin Shen, A Residual Based Kernel Regression Method for Image De-noising, Mathematical Problems in Engineering, (2016) 1–13.

[7] Jianchao Yang, John Wright, Thomas Huang and Yi Ma, Image Super-Resolution via Sparse Representation, IEEE Trans. Image Processing 19 (2010) 2861–2873.

[8] Xiaoyu Wang, Xiaoxu Ou, Bo-Wei Chen, and Mucheol Kim, Image De-noising Based on Improved Wavelet Threshold Function for Wireless Camera Networks and Transmissions, International Journal of Distributed Sensor Networks (2015) 1–8.

[9] Kostadin Dabov, Alessandro Foi, Vladimir Katkovnik and Karen Egiazarian, Image De-noising by Sparse 3D Transform-domain Collaborative Filtering, IEEE Transaction on Image Processing 16 (2007) 2080–2095.

[10] X. P. Zhang, Space Scale Adaptive Noise Reduction in Images based on Thresholding Neural Network. In: Proceeding of IEEE International Conference on Acoustics, Speech and Signal Processing, vol. 3, Salt Lake City, UT, May 7–11 (2001).

[11] Noorbakhsh Amiri Golilarz, Niyifasha Robert and Jalil Addeh, Survey of Image De-noising using Wavelet Transform Combined with Thresholding Functions, Computational Research Progress in Applied Science and Engineering (CRPASE) 3 (2017) 132–135.